

Optimization of grid design for solar cells

Liu Wen(刘雯), Li Yueqiang(李越强), Chen Jianjun(陈建军), Chen Yanling(陈燕凌),
Wang Xiaodong(王晓东)[†], and Yang Fuhua(杨富华)

(Engineering Research Center for Semiconductor Integrated Technology, Institute of Semiconductors,
Chinese Academy of Sciences, Beijing 100083, China)

Abstract: By theoretical simulation of two grid patterns that are often used in concentrator solar cells, we give a detailed and comprehensive analysis of the influence of the metal grid dimension and various losses directly associated with it during optimization of grid design. Furthermore, we also perform the simulation under different concentrator factors, making the optimization of the front contact grid for solar cells complete.

Key words: grid contact; losses; concentrator solar cells; concentrator factor; simulation

DOI: 10.1088/1674-4926/31/1/014006 **EEACC:** 2560

1. Introduction

Solar energy power generation technology has become an important topic in solving the future energy problem. The key issues in generalizing this technology are improving the conversion efficiency and reducing the price per peak watt of energy obtained in this way. The improvement of a solar cell's efficiency not only depends on materials and structure; it is also very important to optimize the front metal grid design. Especially in concentrator solar cells, too narrow or too wide a spacing between grid lines can both cause large power loss as the current density generated by such a cell is so high. If the spacing is too narrow, the loss of the grid shadowing will be larger, whereas, if the spacing is too wide, the loss of series resistance will be larger. The losses associated with the grid directly influence the conversion efficiency of solar cells.

There are four loss mechanisms directly associated with the grid: (1) grid-metal resistance; (2) shadowing loss due to grid reflection; (3) emitting layer resistance; (4) contact resistance between the metal and the semiconductor. Although the literature about optimizing the grid design is plentiful^[1-8], detailed and comprehensive analyses on the influence of each part of the loss are rare. In the present work, on a theoretical basis, specific and detailed analyses are given by theory simulation for two different top contact grid structures that are usually used in concentrator solar cells.

2. Basic theories

Theories of grid design optimization have already been subject to a great deal of analysis in the literature^[1-4]. Here, we develop a foolproof discussion on the basis of them. First of all, as the current density is proportional to the intensity of the light incident on the cell and the area of the cell exposed to the light, the collecting bus can be located outside the illuminated area and its contribution to the losses can be negligible. So next, we just talk about the losses related to the grid line. In

Ref. [1], these losses are given by Eqs. (1)–(4):

$$P_{rf} = \frac{1}{m} B^2 \rho_{smf} \frac{J_{mp}}{V_{mp}} \frac{S}{W_F}, \quad (1)$$

$$P_{sf} = \frac{W_F}{S}, \quad (2)$$

$$P_{cf} = \rho_M \frac{J_{mp}}{V_{mp}} \frac{S}{W_F}, \quad (3)$$

$$P_{tl} = \frac{\rho_s}{12} \frac{J_{mp}}{V_{mp}} S^2, \quad (4)$$

$$FSUM = P_{rf} + P_{sf} + P_{cf} + P_{tl}, \quad (5)$$

where P_{rf} is the loss due to the series resistance of the metal grid line, P_{sf} is the loss due to the grid shadowing, P_{cf} is the loss due to the contact resistance between the grid lines and the semiconductor, P_{tl} is the loss due to the lateral current flow in the top diffused layer, FSUM is the total loss, B is the dimension of the divided sub-cells, J_{mp} and V_{mp} are the maximum current density and voltage, ρ_{smf} is the sheet resistance of the metal grid, W_F and S are the width of the grid line and the distance between two fingers in the grid, ρ_c is the contact resistance, and ρ_s is the sheet resistance of the emitter layer. If every part of the grid is uniform, m is 3; if not, m is 4.

The specific method for optimizing the metal grid is as follows. First the width of the grid fingers is fixed by the limitation of the technical process; then, according to this value, we can get the value of S by Eq. (6); finally, taking $S_0 = S/2$ as the initial value, Equation (7) can be iterated and S can be converged to a constant value S_{opt} .

$$\frac{W_F}{S} = B \sqrt{\frac{\rho_{smf} + \rho_c m / B^2}{m} \frac{J_{mp}}{V_{mp}}}, \quad (6)$$

$$S_i = \frac{S_{i-1}(3P_{sf} - P_{rf} - P_{cf})}{2(P_{sf} + P_{tl})}, \quad i = 1, 2, 3, \dots \quad (7)$$

When the thickness of the grid finger is involved, according to the theory analyses from Ref. [2], the loss due to the series

[†] Corresponding author. Email: xdwang@semi.ac.cn

Received 6 July 2009

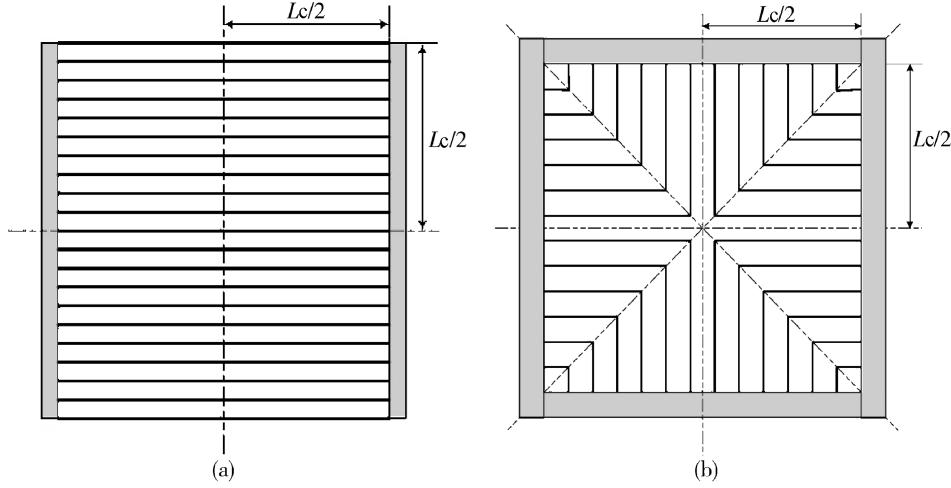


Fig. 1. Two typical top contact grid patterns. (a) Linear grid configuration. (b) Inverted square symmetry grid configuration (square grid for short).

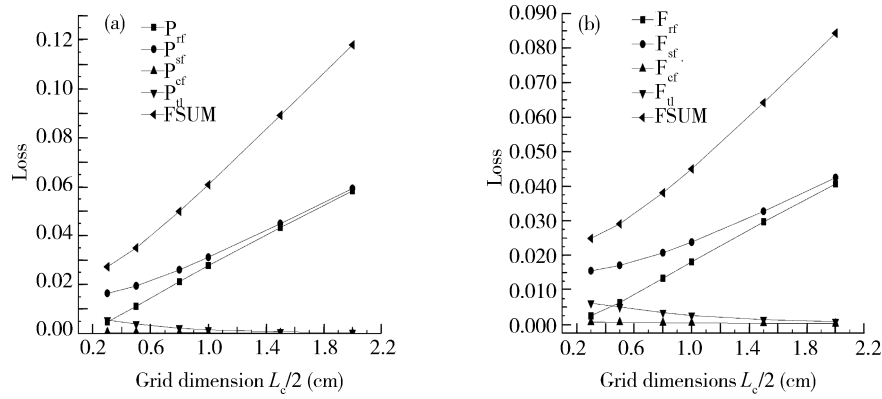


Fig. 2. Optimum value of each part of the loss and FSUM for different L_c values. (a) Linear grid configuration. (b) Inverted square grid symmetry configuration.

resistance of the metal grid line is

$$F_{LD} = \frac{n J_m \rho_M L_c / 2^2}{12 V_m S^2 L_{fg}}, \quad (8)$$

where $n = W_{fg}/t$, and is generally taken as 4. t and W_{fg} are the thickness and width of the grid finger, ρ_M is the resistivity of the metal grid line, $S = W_{fg}/L_{fg}$, and L_{fg} is the distance between two grid fingers. Comparing and contrasting Eqs. (1) and (8), it can be found that Equations (1) and (8) are the same if letting $m = 3, n = 4$, so actually the thickness of the grid finger can be taken as a quarter of the width of the grid line.

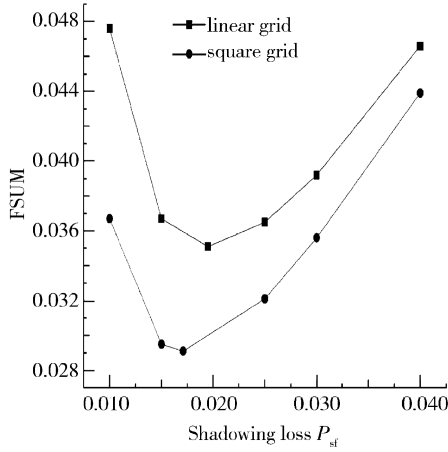
3. Simulation analyses

Figures 1(a) and 1(b) give two typical top contact grid structures that are used in concentrator solar cells. For the expression for each part of the loss, refer to Ref. [2]. Equations (1)–(7) can be solved numerically using the computer program MATLAB and the parameters are shown in Table 1. In the following discussion, the relevant parameters will be changed when we talk about the influence of different parameters. At the same time, in order to complement our visualization, we give more intuitive analyses in the figures.

First the influences of different grid dimensions are studied. The variations in each optimized part of the loss and FSUM for different cell areas are shown in Figs. 2(a) and 2(b). From Figs. 2(a) and 2(b), it should be noted that the two bigger losses are P_{rf} and P_{sf} which increase with the grid dimension. Furthermore, P_{rf} shows a very obvious increase and is close to P_{sf} with the increase of the cell area. The optimized P_{tl} shows a small decrease with the increment of the grid dimension and P_{cf} as the smallest loss remains approximately constant. However, comparing these two pictures, every loss except P_{cf} of the square grid is lower than the loss of the linear grid. This is why the square grid is superior to the linear grid, especially for large area solar cells.

At the same time, Figures 2(a) and 2(b) also show that with increasing solar cell area, the main measure to optimize the grid pattern is to decrease P_{rf} and P_{sf} .

As P_{sf} and P_{rf} are the major parts of the total loss, specific analyses are given here. Figure 3 shows the variation of FSUM for two grid patterns against the shadowing loss P_{sf} . It is obvious that, for the same value of P_{sf} , the FSUM of the square grid is less than that of the linear grid. There is also an optimum value of P_{sf} which makes the FSUM value smallest. When P_{sf} is below this value, FSUM shows an obvious increase with de-

Fig. 3. Value of FSUM for different P_{sf} values.

creasing P_{sf} ; when P_{sf} is above this value, the increment of FSUM is relatively small with the increase of P_{sf} . This also shows that the value of P_{sf} should be optimum. Otherwise, it can be selected bigger rather than smaller; if not, the total loss FSUM will be bigger.

Figures 4(a) and 4(b) show the variation in optimum losses for the two grid patterns against the resistivity of the metal grid. From Fig. 4(a) it can be seen that the optimum P_{rf} and the biggest loss P_{sf} has a small increment with increasing metal grid resistivity; however, P_{tl} has a small decrement. These variations are more sensitive to the linear grid pattern, especially for P_{rf} . It can also be seen that the ohmic contact losses of the two grid patterns show little change and are almost the same. From Fig. 4(b) it can be seen that, although the total loss of a grid pattern increases with metal finger resistivity, as expected, the square grid is less sensitive to this variation.

Now we will give a brief explanation of the influence of ohmic contact (see Fig. 5). Because P_{cf} is almost the same for the two top contact grid patterns, here only the linear grid pattern is discussed. It is clear from Fig. 5 that the optimized P_{cf} , P_{sf} and FSUM increase with increasing ρ_c when its value is above $1 \times 10^{-4} \Omega \cdot \text{cm}^2$, while the optimized P_{rf} and P_{tl} decrease. In particular, when ρ_c is above $1 \times 10^{-3} \Omega \cdot \text{cm}^2$, these increments and decrements are dramatic. However, if ρ_c is below $1 \times 10^{-4} \Omega \cdot \text{cm}^2$, it should be noted that all the optimized losses are almost constant and P_{cf} is close to zero, so the power loss brought by the ohm contact can be neglected. Actually, this value can be achieved easily in experiment.

Furthermore, as the optimization of the front contact grid pattern in concentrator solar cells is more important, we discuss the optimization at different concentrator factors. First of all, referring to Ref. [9], the optimum current density, optimum voltage, and conversion efficiency under different concentrator factors are given in Eqs. (9)–(11):

$$J_M(C) = C J_M(1), \quad (9)$$

$$V_M(C) = V_M(1) + \frac{kT}{q} \ln C, \quad (10)$$

$$\eta(C) = \frac{J_M(C)V_M(C)}{0.1C}(1 - \text{FSUM}), \quad (11)$$

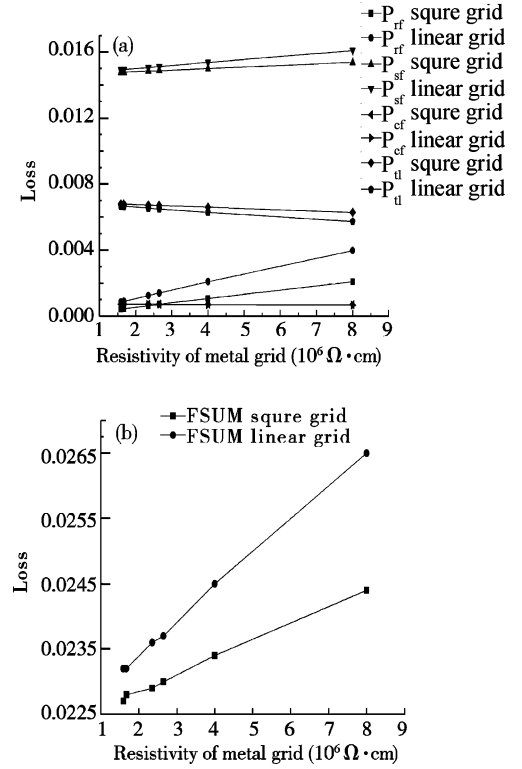
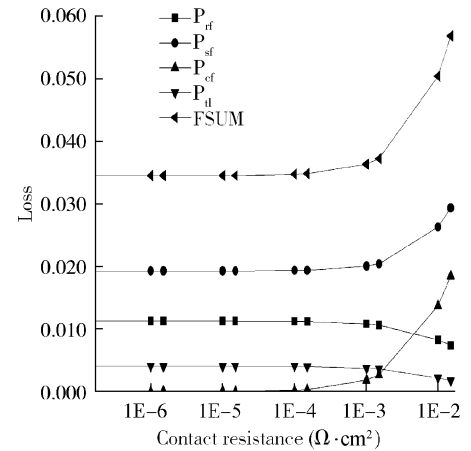


Fig. 4. (a) Each optimized part of the loss for the two grid patterns against metal grid resistivity. (b) Optimized FSUM for the two grid patterns against metal grid resistivity.

Fig. 5. Losses for different values of contact resistance ρ_c in the linear grid pattern.

where $J_M(1)$ and $V_M(1)$ are the optimum current density and optimum voltage at 1 sun, C is the concentrator factor, and T is the temperature of the solar cell and is assumed constant at 300 K. The parameters are just the same as in Table 1.

The variation with concentrator factor of all the optimized power losses and conversion efficiency for the two grid patterns is shown in Figs. 6(a) and 6(b). It is obvious that with the increment of C , all the power losses after optimization increase. Moreover, the linear grid is more sensitive to this variation. This means that the square grid is preferable to the linear grid with the increment of C . From Fig. 6(b) it can be observed that the optimum concentrator factor is about 5 suns and the

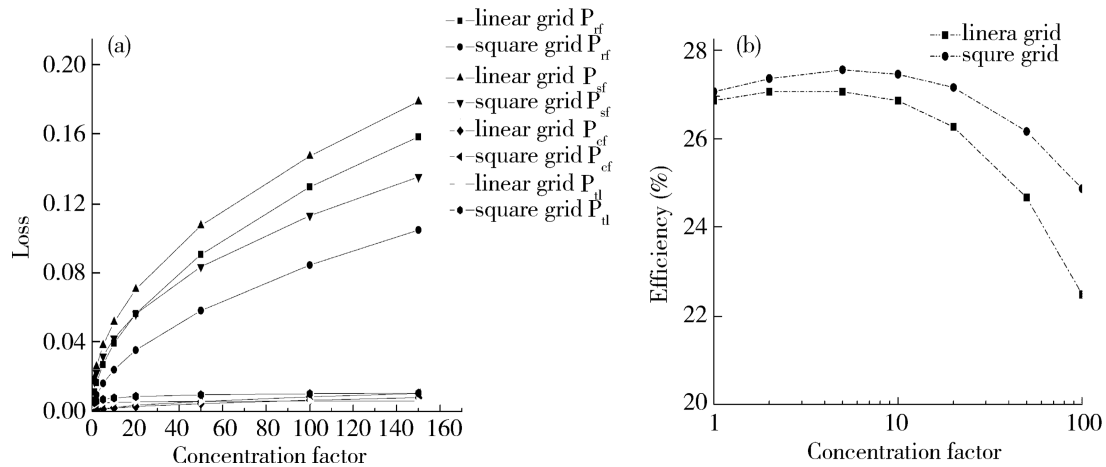


Fig. 6. (a) All the calculated power losses at different concentration factors for the linear and square grids. (b) Conversion efficiency at different concentration factors for the linear and square grids.

Table 1. Solar cell parameters.

Parameter	Value
L_c	1 cm
W_F	15 μm
J_m	31.7 mA/cm ²
V_m	880 mV
ρ_c	$3 \times 10^{-4} \Omega \cdot \text{cm}^2$
ρ_s	220 Ω/\square
$\rho_M(\text{Ag})$	$7.2 \times 10^{-2} \Omega/\square$

less efficient it is, the higher the concentrator factor becomes. This is just because that with the increment of C , the power dissipated by the series resistance is also larger. However, we can obtain the optimum conversion efficiency by selecting the optimum shadowing loss and sunlight concentration factor using a simulation of optimum grid pattern and concentrator factor.

4. Conclusion

By investigating two typical top contact grid structures used in concentrator solar cells, specific and detailed analyses were given in this work of the influence of dimension, resistivity, shadowing loss, and ohmic contact resistance of the metal grid during grid pattern optimization, and the two grid patterns were contrasted. We found that with increasing solar cell area, it was more important to optimize the grid pattern and the main measure to take was to decrease loss due to the grid finger resistance and shadowing loss. For shadowing loss, it was better to select either the optimum value or one little larger rather than

smaller; if not, the losses would be bigger. However, the loss due to ohm contact could be neglected if the contact resistance was below $1 \times 10^{-4} \Omega \cdot \text{cm}^2$. In experiment, this value could be easily obtained. Furthermore, to make the optimization of the front contact grid for solar cells more complete, we simulated the optimization of the front grid and conversation efficiency for concentrator solar cells at different concentrator factors.

References

- [1] Green M A. Solar cells operating principles, technology, and system applications. Beijing: Publishing House of Electronics Industry, 1987
- [2] Moore A R. An optimized grid design for a sun-concentrator solar cell. RCA Review, 1979, 40: 140
- [3] Flat A, Milnes A G. Optimization of multi-layer front-contact grid patterns for solar cells. Sol Energy, 1979, 23: 289
- [4] Shabana M M. Optimization of grid design for solar cells at different illumination levels. Sol Cells, 1989, 26: 177
- [5] Gangopadhyay U, Saha H, Dutta S K. Front grid design for plated contact solar cell. Conference Record of the 29th IEEE Photovoltaic Specialists, 2002
- [6] Shen Lanxian, Chen Tingjin, Liu Zuming. The analysis and preparation of silicon solar cells contact system. Journal of Yunnan Normal University, 2006, 26(5): 25
- [7] Shi Xiaozhong, Wang Le, Xia Guanqun. The grid-lines design of solar cells. Acta Electronica Sinica, 1999, 27(11): 126
- [8] Morillo P, Bobeico E, Formisano F, et al. Influence of metal grid patterns on the performance of silicon solar cells at different illumination levels. Mater Sci Eng B, 2009, 159/160: 318
- [9] Morales-Acevedo A. Optimum concentration factor for silicon solar cells. Sol Cells, 1985, 14: 43